Worst-Case Finite-Frequency H 2 -Norm Analysis of Uncertain Linear Systems

Tommaso Casati, Jean-Marc Biannic, Clément Roos, Hélène Evain

Worst-Case Finite-Frequency H_2-Norm Analysis of Uncertain Linear Systems

Tommaso Casati * **Jean-Marc Biannic** * **Clément Roos** *
Hélène Evain **

* *DTIS, ONERA, Université de Toulouse, 31000 Toulouse France (e-mails: {tommaso.casati, clement.roos, jean-marc.biannic}@onera.fr)*
** *CNES - The French Space Agency, 31400 Toulouse France (e-mail: helene.evain@cnes.fr)*

Abstract: The H_2 norm is a fundamental design metric in many control applications and it is therefore important to evaluate how it is affected by uncertainties in the model. In the space domain, the H_2 norm is particularly significant when the Pointing Error Source (PES) of a satellite can be approximated by a white noise, which is often the case for microvibrations and acoustic disturbances. The present paper discusses a new method to identify a set of real parametric uncertainties which maximizes (resp. minimizes) the finite-frequency H_2 norm of an uncertain Multiple-Input Multiple-Output (MIMO) linear system. To do so, the analytical expression of the finite-frequency H_2 norm is first approximated as a sum of contributions on a discrete frequency grid. A constrained nonlinear optimization is then performed to maximize (resp. minimize) the so-obtained function. The proposed worst-case finite-frequency H_2-norm analysis paves the way to a wide range of possible applications, specially when integrated into the Verification and Validation (V&V) process of space missions requiring high pointing performances. The theoretical results derived in the paper are implemented and successfully tested on models of increasing complexity.

Keywords: H_2 norm; uncertain systems; robustness analysis; constrained nonlinear optimization; worst-case uncertainty; space applications.

1. INTRODUCTION

The H_2 norm represents a pivotal design metric in many control applications (see e.g. Garulli et al. (2013) and references therein). This norm, in fact, corresponds to the ℓ_2 norm of the impulse response and to the Root Mean Square (RMS) norm of the system's output when the input is a white noise. In space applications, the H_2 norm becomes a relevant metric when the Pointing Error Source (PES) of a satellite can be approximated by a white noise, which is often the case of microvibrations and acoustic disturbances. In this context, furthermore, the increasing need for high pointing performance missions with reduced development times requires efficient Verification and Validation (V&V) techniques to assess the robustness of the Attitude and Orbit Control System (AOCS) as early as possible in the design procedure. It is therefore important to evaluate how the H_2 norm is affected by uncertainties in the model.

Different approaches have been discussed in the literature to compute a guaranteed upper bound on the H_2 norm that can be reached by an uncertain linear system. In this field, a relevant method was proposed by Paganini (1999) based on SemiDefinite Programs (SDPs) subject to Linear Matrix Inequalities (LMIs). In practice, the problem was solved on a finite frequency grid and a Hamiltonian-based technique inspired by Ferreres (1998) was then used by Garulli et al. (2013) to validate the results on the entire frequency range. A similar approach was also proposed by Casati et al. (2024) to compute guaranteed lower bounds on the robust finite-frequency H_2 norm of an uncertain system. All these methods, however, only provide guaranteed bounds on the performance, which do not correspond to feasible configurations of the uncertain system. On the contrary, the worst-case finite-frequency H_2-norm analysis aims to determine the combinations of uncertainties for which the finite-frequency H_2 norm of a model is maximum. Such an analysis would entail remarkable benefits when integrated into the V&V process of space missions requiring high pointing performances. A fast detection of worst-case finite-frequency H_2-norm conditions could in fact guide Monte Carlo simulations towards critical configurations, increasing the effectiveness of the test campaigns and lightening the validation procedure. Furthermore, a robust multimodel design of the AOCS could be tackled yet in the early phases of the control synthesis by imposing an H_2-norm performance requirement directly on the system realization with the worst-case combination of uncertainties.

In this context, an interesting approach was proposed by Patartics et al. (2023) to construct worst-case uncertainties such that the gain of a system is maximized at multiple frequencies. The method can deal with both dynamic uncertainties, constructed through the boundary Nevanlinna–Pick interpolation, and parametric uncertain-

ties. The optimization was performed by a standard interior point algorithm implemented in the function *fmincon* from the Matlab Optimization toolbox. The objective function was defined so as to maximize the largest singular value of the transfer function on a grid of frequencies. This research, however, was not specifically conceived for H_2-norm analysis and it cannot be directly used to assess the robust H_2 performance of Multiple-Input Multiple-Output (MIMO) systems. Similar optimization-based techniques were also used by Biannic et al. (2016) in the context of μ-analysis to compute worst-case perturbations. The problem was formulated as a constrained nonlinear optimization (see e.g. Brito and Kim (2010); Yazıcı et al. (2011)), which can be solved with standard tools such as *fmincon*. Martin et al. (2021), furthermore, proposed a sampling-based technique to identify the worst-case H_2 norm of an uncertain system. This approach, however, becomes time-consuming when the number of uncertainties increases and may fail to detect rare events.

The present paper proposes a new approach to perform the worst-case finite-frequency H_2-norm analysis of uncertain linear systems in the presence of real parametric LTI uncertainties. In practice, the analytical expression of the finite-frequency H_2 norm is first approximated as a sum of contributions computed on a frequency grid. Then, a constrained nonlinear optimization technique is adopted to search for a maximum of the so-obtained function with respect to a set of real parametric uncertainties. The proposed approach is particularly interesting for different reasons. First, differently from Patartics et al. (2023), the optimization is performed on the trace of the system's transfer matrix (and not on its maximum singular value). This makes our method equivalently valid for both Single-Input Single-Output (SISO) and MIMO systems. Furthermore, despite the fact that the resulting maxima may be only locally optimal, the implemented algorithm always yields a feasible realization of the uncertain system. Eventually, the proposed approach can easily be extended to compute best-case finite-frequency H_2-norm conditions, namely to identify a set of uncertainties for which the finite-frequency H_2 norm of an uncertain system is minimum. The so-obtained worst and best-case finite-frequency H_2-norm values may therefore be respectively compared with the guaranteed upper and lower bounds of Casati et al. (2024), providing precious information on their accuracy.

The paper is organized as follows. Some preliminaries to the worst-case finite-frequency H_2-norm performance problem are first discussed in Section 2. Analytical expressions for the gradient and the Hessian matrix of the finite-frequency H_2 norm with respect to a set of real parametric uncertainties are then presented in Section 3. Eventually, the theoretical results are implemented in Section 4 and applied to examples of increasing complexity in Section 5.

Notation

The notation used in the paper is standard. Bold font is adopted for vectors and matrices, whereas roman characters indicate scalars. Given a matrix $\boldsymbol{A}$, $\boldsymbol{A}^*$ is its conjugate transpose and $\mathrm{tr}\,(\boldsymbol{A})$ its trace. $\boldsymbol{I}$ stands for the identity matrix. Given n matrices $\{\boldsymbol{A}_i\}_{i=1,\dots,n}$, $\mathrm{diag}\,(\boldsymbol{A}_1,\dots,\boldsymbol{A}_n)$ denotes the standard block-diagonal augmentation. $||\cdot||_\infty$ and $||\cdot||_2$ indicate the H_∞ norm and the H_2 norm respectively. Open intervals are delimited by parentheses $(\cdot)$, whereas closed intervals are bounded by brackets $[\cdot]$. The absolute value of a number is denoted by abs.

2. PRELIMINARY CONSIDERATIONS

2.1 Definitions

Consider the uncertain continuous-time robustly-stable MIMO linear system of Fig. 1, where the transfer matrix between $\boldsymbol{u}$, of size r, and $\boldsymbol{y}$, of (possibly) different size l, corresponds to the upper well-posed Linear Fractional Transformation (LFT) $\boldsymbol{\mathcal{F}}_u\left(\boldsymbol{M}\left(s\right),\boldsymbol{\Delta}\right)$.

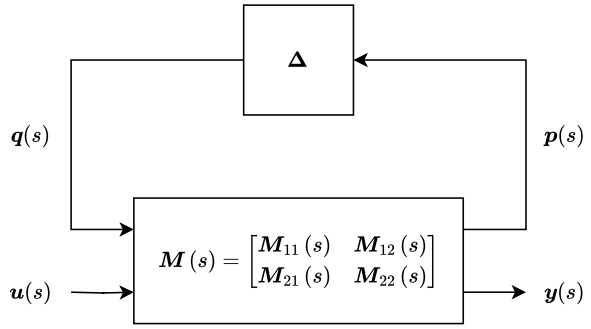

Fig. 1. LFT representation of an uncertain continuous-time MIMO system.

$\boldsymbol{M}\left(s\right)=\begin{bmatrix}\boldsymbol{M}_{11}\left(s\right) & \boldsymbol{M}_{12}\left(s\right)\\ \boldsymbol{M}_{21}\left(s\right) & \boldsymbol{M}_{22}\left(s\right)\end{bmatrix}$ is a continuous-time, stable and proper real-rational transfer function representing the nominal closed-loop system. $\boldsymbol{\Delta}=\mathrm{diag}\left(\boldsymbol{\Delta}_1,\dots,\boldsymbol{\Delta}_{n_u}\right)$ is a structured diagonal LTI operator which gathers all n_u model uncertainties. Each $\boldsymbol{\Delta}_i$, furthermore, is assumed to be a diagonal matrix $\boldsymbol{\Delta}_i=\delta_i\boldsymbol{I}_{m_i}$ of size $m_i\times m_i$ where δ_i is a real parametric uncertainty and m_i its number of occurrences (Roos, 2018). Let $\boldsymbol{D}_\Delta$ be the set of admissible uncertainties, i.e. the set of all uncertainties $\boldsymbol{\Delta}$ with the size and structure defined above. Let then $\boldsymbol{B}_\Delta=\{\boldsymbol{\Delta}\in\boldsymbol{D}_\Delta:||\boldsymbol{\Delta}||_\infty\leq 1\}$ be the associated unit ball. For any admissible $\boldsymbol{\Delta}\in\boldsymbol{D}_\Delta$, the finite-frequency H_2 norm of the transfer matrix $\boldsymbol{\mathcal{F}}_u\left(\boldsymbol{M}\left(s\right),\boldsymbol{\Delta}\right)$ is defined as

$$||\boldsymbol{\mathcal{F}}_u\left(\boldsymbol{M}\left(s\right),\boldsymbol{\Delta}\right)||_{2,\overline{\omega}}^2:=\int_0^{\overline{\omega}}\mathrm{tr}\left(\boldsymbol{\mathcal{F}}_u\left(j\omega\right)\boldsymbol{\mathcal{F}}_u\left(j\omega\right)^*\right)\frac{d\omega}{\pi} \tag{1}$$

where $\boldsymbol{\mathcal{F}}_u\left(j\omega\right)$ is written instead of $\boldsymbol{\mathcal{F}}_u\left(\boldsymbol{M}\left(j\omega\right),\boldsymbol{\Delta}\right)$ to simplify the notation and $\overline{\omega}\in[0,+\infty)$ (Garulli et al., 2013). If $\overline{\omega}=+\infty$, the classical definition of H_2 norm is obtained, in which case $\boldsymbol{\mathcal{F}}_u\left(\boldsymbol{M}\left(s\right),\boldsymbol{\Delta}\left(s\right)\right)$ is assumed strictly proper. Note that in practical applications, the identified models are usually valid at low frequencies until a given threshold. The finite-frequency H_2 norm therefore captures the uncertain system's behavior in its representative region.

2.2 Problem Formulation

A method is proposed to identify a feasible combination of uncertainties that yields the largest (resp. lowest) finite-frequency H_2 norm of an uncertain linear system. For-

mally, this corresponds to compute $\boldsymbol{\Delta}_{wc}$ (resp. $\boldsymbol{\Delta}_{bc}$) such that

$$\boldsymbol{\Delta}_{wc} = \underset{\boldsymbol{\Delta}\in\boldsymbol{B}_{\Delta}}{\arg\max}\, ||\boldsymbol{\mathcal{F}}_u(\boldsymbol{M}(s),\boldsymbol{\Delta})||_{2,\overline{\omega}} \tag{2}$$

$$\boldsymbol{\Delta}_{bc} = \underset{\boldsymbol{\Delta}\in\boldsymbol{B}_{\Delta}}{\arg\min}\, ||\boldsymbol{\mathcal{F}}_u(\boldsymbol{M}(s),\boldsymbol{\Delta})||_{2,\overline{\omega}} \tag{3}$$

3. GRADIENT AND HESSIAN OF THE FINITE-FREQUENCY H_2 NORM

Before discussing the implemented method to perform the constrained nonlinear optimization of (2) (resp. (3)), this section introduces analytical expressions for both the gradient and the Hessian matrix of the finite-frequency H_2 norm with respect to a set of real parametric uncertainties. Letting $\boldsymbol{\Lambda} = (\boldsymbol{I} - \boldsymbol{M}_{11}\boldsymbol{\Delta})^{-1}$ and recalling (1), the finite-frequency H_2 norm of the LFT represented in Fig. 1 can be expressed as

$$||\boldsymbol{\mathcal{F}}_u(\boldsymbol{M}(s),\boldsymbol{\Delta})||^2_{2,\overline{\omega}} = \int_0^{\overline{\omega}} \mathrm{tr}\big((\boldsymbol{M}_{22}+\boldsymbol{M}_{21}\boldsymbol{\Delta}\boldsymbol{\Lambda}\boldsymbol{M}_{12}) \cdot (\boldsymbol{M}_{22}+\boldsymbol{M}_{21}\boldsymbol{\Delta}\boldsymbol{\Lambda}\boldsymbol{M}_{12})^*\big)\frac{d\omega}{\pi}$$

Note that for the properties of transpose conjugation, the relation $\boldsymbol{\Lambda}^* = (\boldsymbol{I} - \boldsymbol{\Delta}\boldsymbol{M}_{11}^*)^{-1}$ holds. Let now $\tilde{\boldsymbol{\Delta}}_i = \dfrac{\partial}{\partial\delta_i}\boldsymbol{\Delta}$ be the derivative of $\boldsymbol{\Delta}$ with respect to an uncertainty δ_i. As all the uncertain parameters are assumed independent of each other, it holds that $\tilde{\boldsymbol{\Delta}}_i = \mathrm{diag}\left(\boldsymbol{0}_{m_1},\ldots,\boldsymbol{I}_{m_i},\ldots,\boldsymbol{0}_{m_{n_u}}\right)$. By computing the derivative of (1) with respect to each uncertainty, it is then possible to construct the gradient $\boldsymbol{\nabla}\left(||\boldsymbol{\mathcal{F}}_u(\boldsymbol{M}(s),\boldsymbol{\Delta})||_{2,\overline{\omega}}\right)$ of the finite-frequency H_2 norm as

$$\boldsymbol{\nabla}\left(||\boldsymbol{\mathcal{F}}_u(\boldsymbol{M}(s),\boldsymbol{\Delta})||_{2,\overline{\omega}}\right) = \begin{bmatrix} \dfrac{\partial}{\partial\delta_1}||\boldsymbol{\mathcal{F}}_u(\boldsymbol{M}(s),\boldsymbol{\Delta})||_{2,\overline{\omega}} \\ \vdots \\ \dfrac{\partial}{\partial\delta_{n_u}}||\boldsymbol{\mathcal{F}}_u(\boldsymbol{M}(s),\boldsymbol{\Delta})||_{2,\overline{\omega}} \end{bmatrix}$$

The Hessian matrix $\boldsymbol{H}\left(||\boldsymbol{\mathcal{F}}_u(\boldsymbol{M}(s),\boldsymbol{\Delta})||_{2,\overline{\omega}}\right)$ of the finite-frequency H_2 norm can successively be derived as

$$\boldsymbol{H}\left(||\boldsymbol{\mathcal{F}}_u(\boldsymbol{M}(s),\boldsymbol{\Delta})||_{2,\overline{\omega}}\right) = \mathrm{diag}\left(\begin{bmatrix} \dfrac{\partial^2}{\partial\delta_1^2}||\boldsymbol{\mathcal{F}}_u(\boldsymbol{M}(s),\boldsymbol{\Delta})||_{2,\overline{\omega}} \\ \vdots \\ \dfrac{\partial^2}{\partial\delta_{n_u}^2}||\boldsymbol{\mathcal{F}}_u(\boldsymbol{M}(s),\boldsymbol{\Delta})||_{2,\overline{\omega}} \end{bmatrix}\right)$$

The gradient and the Hessian matrix of (1) are then used in Section 4 to perform the constrained nonlinear optimization of (2) (resp. (3)).

4. IMPLEMENTED ALGORITHM

The rigorous computation of the finite-frequency H_2 norm and its derivatives requires solving an integral between 0 and $\overline{\omega}$. In practice, the optimization is performed using the finite-frequency H_2-norm approximating function $f(\boldsymbol{\Delta})$ such that

$$||\boldsymbol{\mathcal{F}}_u(\boldsymbol{M}(s),\boldsymbol{\Delta})||^2_{2,\overline{\omega}} \approx f(\boldsymbol{\Delta}) = \sum_{k=1}^{N} \mathrm{tr}\left(\boldsymbol{\mathcal{F}}_u(j\omega_k)\boldsymbol{\mathcal{F}}_u(j\omega_k)^*\right)\frac{\mathrm{length}\left(I(\omega_k)\right)}{\pi}$$

where $\{\omega_k\}_{k=1,\ldots,N}$ is a set of N frequency grid points and $I(\omega_k)$ are N disjoint frequency intervals such that $\omega_k \in I(\omega_k)$ and $\bigcup_{k=1}^{N} I(\omega_k) \equiv [0,\overline{\omega}]$. Similarly, the derivative of the finite-frequency H_2 norm with respect to an uncertainty δ_i is approximated as the derivative of $f(\boldsymbol{\Delta})$ with respect to δ_i:

$$\frac{\partial}{\partial\delta_i}||\boldsymbol{\mathcal{F}}_u(\boldsymbol{M}(s),\boldsymbol{\Delta})||^2_{2,\overline{\omega}} \approx \frac{\partial}{\partial\delta_i}f(\boldsymbol{\Delta}) = \sum_{k=1}^{N} \mathrm{tr}\left(\frac{\partial}{\partial\delta_i}\left(\boldsymbol{\mathcal{F}}_u(j\omega_k)\boldsymbol{\mathcal{F}}_u(j\omega_k)^*\right)\right)\frac{\mathrm{length}\left(I(\omega_k)\right)}{\pi} \tag{4}$$

The same consideration holds for the second derivative of the finite-frequency H_2 norm with respect to δ_i:

$$\frac{\partial^2}{\partial\delta_i^2}||\boldsymbol{\mathcal{F}}_u(\boldsymbol{M}(s),\boldsymbol{\Delta})||^2_{2,\overline{\omega}} \approx \frac{\partial^2}{\partial\delta_i^2}f(\boldsymbol{\Delta}) = \sum_{k=1}^{N} \mathrm{tr}\left(\frac{\partial^2}{\partial\delta_i^2}\left(\boldsymbol{\mathcal{F}}_u(j\omega_k)\boldsymbol{\mathcal{F}}_u(j\omega_k)^*\right)\right)\frac{\mathrm{length}\left(I(\omega_k)\right)}{\pi} \tag{5}$$

A constrained nonlinear optimization problem is then solved to find a feasible set of uncertainties $\boldsymbol{\Delta}_{wc}$ for which the approximated finite-frequency H_2 norm of an uncertain system is maximum:

$$\boldsymbol{\Delta}_{wc} = \underset{\boldsymbol{\Delta}\in\boldsymbol{B}_{\Delta}}{\arg\max}\, f(\boldsymbol{\Delta}) \tag{6}$$

Analogously, the best-case analysis aims to determine a feasible set of uncertainties $\boldsymbol{\Delta}_{bc}$ for which the approximated finite-frequency H_2 norm of an uncertain system is minimum:

$$\boldsymbol{\Delta}_{bc} = \underset{\boldsymbol{\Delta}\in\boldsymbol{B}_{\Delta}}{\arg\min}\, f(\boldsymbol{\Delta}) \tag{7}$$

The constrained nonlinear optimization can be performed using the MATLAB built-in function *fmincon*. In the following, however, another simple algorithm is proposed in addition to *fmincon*. As highlighted in Section 5, the main advantage of this additional method is that it yields the same results as *fmincon* in a lower computational time. This fact is particularly significant in the perspective of the algorithm being included into a Branch and Bound (B&B) scheme to perform probabilistic H_2-norm analysis. In this case, in fact, the computation of worst (resp. best) conditions may be repeated thousands of times, causing an exponential increase in the computational burden.

The implemented iterative procedure, based on the Newton's method, computes new guesses δ_i^{NEW}, $i = 1,\ldots,n_u$ from the previous-iteration set of uncertainties $\boldsymbol{\Delta}^{OLD} = \mathrm{diag}\left(\delta_1^{OLD}\boldsymbol{I}_{m_1},\ldots,\delta_i^{OLD}\boldsymbol{I}_{m_i},\ldots,\delta_{n_u}^{OLD}\boldsymbol{I}_{m_{n_u}}\right)$. To do so, at each iteration the following Newton's step is consecutively evaluated n_u times, once for each uncertain parameter δ_i, assumed independent of the others:

$$\delta_i^{NEW} = \delta_i^{OLD} - \left(\frac{\partial^2}{\partial\delta_i^2}f(\boldsymbol{\Delta})\bigg|_{\boldsymbol{\Delta}=\boldsymbol{\Delta}^{OLD}}\right)^{-1}\frac{\partial}{\partial\delta_i}f(\boldsymbol{\Delta})\bigg|_{\boldsymbol{\Delta}=\boldsymbol{\Delta}^{OLD}} \tag{8}$$

If $\dfrac{\partial^2}{\partial\delta_i^2}f(\boldsymbol{\Delta})\bigg|_{\boldsymbol{\Delta}=\boldsymbol{\Delta}^{OLD}}$ is not invertible, (8) is replaced by a gradient step. The algorithm stops when either the gradient of $f(\boldsymbol{\Delta})$ is sufficiently close to $\boldsymbol{0}$ or a corner of the uncertainty domain is reached. Indicating with $\boldsymbol{\Delta}^{NEW}$ the new set of uncertainties and letting

ϵ be a positive scalar, the first condition can be expressed as $\max_{i=1,\dots,n_u} \text{abs}\left(\frac{\partial}{\partial\delta_i} f(\boldsymbol{\Delta})\Big|_{\boldsymbol{\Delta}=\boldsymbol{\Delta}^{NEW}}\right) < \epsilon$. Supposing that the uncertainties are normalized, furthermore, the second condition can be formulated as $\min_{i=1,\dots,n_u} \text{abs}\left(\delta_i^{NEW}\right) = 1$.

Remark 1. The presented approach cannot distinguish between maxima and minima. In order to avoid this issue, a further operation is introduced. If the direction of the Newton's step decreases (resp. increases) $f(\boldsymbol{\Delta})$ when maximization (resp. minimization) is required, δ_i^{NEW} is set to $\text{sgn}\left(\frac{\partial}{\partial\delta_i} f(\boldsymbol{\Delta})\Big|_{\boldsymbol{\Delta}=\boldsymbol{\Delta}^{OLD}}\right)$ (resp. $-\text{sgn}\left(\frac{\partial}{\partial\delta_i} f(\boldsymbol{\Delta})\Big|_{\boldsymbol{\Delta}=\boldsymbol{\Delta}^{OLD}}\right)$), where sgn indicates the sign function. This is reasonable as the worst (resp. best) conditions are usually found in the corners of $\boldsymbol{B}_\Delta$.

Remark 2. Differently from the H_∞ norm, the H_2 norm of an uncertain system is smooth with respect to the uncertain parameters. No technique is therefore included in the algorithm to treat non-smooth optimizations.

The output of the optimization procedure is a feasible combination of the uncertain parameters. Given a state-space representation of $\boldsymbol{\mathcal{F}}_u\left(\boldsymbol{M}(s), \boldsymbol{\Delta}^{NEW}\right) = \left[\begin{array}{c|c} \boldsymbol{A} & \boldsymbol{B} \\ \hline \boldsymbol{C} & \boldsymbol{D} \end{array}\right]$, the maximized (resp. minimized) finite-frequency H_2 norm of the LFT transfer matrix $\boldsymbol{\mathcal{F}}_u(\boldsymbol{M}(s), \boldsymbol{\Delta})$ can eventually be computed as

$$\left\|\boldsymbol{\mathcal{F}}_u\left(\boldsymbol{M}(s), \boldsymbol{\Delta}^{NEW}\right)\right\|_{2,\overline{\omega}}^2 = \text{tr}\left(\boldsymbol{B}^T \boldsymbol{W}_o \boldsymbol{B}\right) \qquad (9)$$

where $\boldsymbol{W}_o$ is the frequency-limited observability Gramian of the system (see e.g. Garulli et al. (2013)). Even though the algorithm may not converge to the global maximum (resp. minimum) of the objective function, it nonetheless yields a feasible combination of the uncertainties, which corresponds to an inner estimate of the worst (reps. best) finite-frequency H_2 norm. The aforementioned considerations are summarized in Algorithm 1, which is tested on different applications in Section 5.

Algorithm 1: Worst-case finite-frequency H_2-norm analysis of uncertain MIMO linear systems.

Set an initial grid of frequencies $\{\omega_k\}_{k=1,\dots,N}$, with the corresponding $I(\omega_k)$, $k = 1, \dots, N$;
Set an initial guess for $\boldsymbol{\Delta}_{wc}$ (resp. $\boldsymbol{\Delta}_{bc}$);
while $\max_{i=1,\dots,n_u} \text{abs}\left(\frac{\partial}{\partial\delta_i} f(\boldsymbol{\Delta})\Big|_{\boldsymbol{\Delta}=\boldsymbol{\Delta}^{NEW}}\right) > \epsilon$ *or* $\min_{i=1,\dots,n_u} \text{abs}\left(\delta_i^{NEW}\right) < 1$ **do**
  for *each* δ_i, $i = 1, \dots, n_u$ **do**
    Compute $\frac{\partial}{\partial\delta_i} f(\boldsymbol{\Delta})\Big|_{\boldsymbol{\Delta}=\boldsymbol{\Delta}^{OLD}}$ and $\frac{\partial^2}{\partial\delta_i^2} f(\boldsymbol{\Delta})\Big|_{\boldsymbol{\Delta}=\boldsymbol{\Delta}^{OLD}}$ with (4) and (5) respectively;
    Compute δ_i^{NEW} with (8);
  end
end
Compute the finite-frequency H_2 norm of $\boldsymbol{\mathcal{F}}_u\left(\boldsymbol{M}(s), \boldsymbol{\Delta}^{NEW}\right)$ with (9).

5. APPLICATIONS

All results have been obtained with MATLAB on a Windows 10 laptop with a 13$^{\text{th}}$ Gen Intel(R) Core(TM) i5-1345U as CPU and 16 GB of RAM.

5.1 Validation Example

Algorithm 1 is first validated on a SISO continuous-time system taken from Garulli et al. (2013). The LFT has a single normalized real parametric uncertainty with two occurrences in $\boldsymbol{\Delta}$ and the state-space matrices of $\boldsymbol{M}(s)$ are as follows:

$$\boldsymbol{A} = \begin{bmatrix} -2.5 & 0.5 & 0 & -50 & 0 \\ 0 & -1 & 0.5 & 0 & 0 \\ 0 & -0.5 & 0 & 0 & 0 \\ 0 & 0 & 0 & -5 & 100 \\ 0 & 0 & 0 & -100 & 0 \end{bmatrix}, \quad \boldsymbol{B} = \begin{bmatrix} 0.25 & -0.5 & 0 \\ 0 & 0 & 5 \\ 0 & 0 & 0 \\ 0 & 0 & 0 \\ 0 & 0 & 5 \end{bmatrix}$$

$$\boldsymbol{C} = \begin{bmatrix} 1 & 0 & 0 & 0 & 0 \\ 0 & 0 & 0 & 0 & 0 \\ 1 & 0 & 0 & 0 & 0 \end{bmatrix}, \quad \boldsymbol{D} = \begin{bmatrix} 0 & 0 & 0 \\ 1 & 0 & 0 \\ 0 & 0 & 0 \end{bmatrix}$$

Choosing $\overline{\omega} = 50\,\text{rad/s}$ and setting $\{\omega_k\}_{k=1,\dots,N}$ to be the middle frequencies of $N = 10$ equispaced intervals $I(\omega_k)$ between $0\,\text{rad/s}$ and $\overline{\omega}$, *fmincon* and Algorithm 1 are run twice to compute both the worst and best-case finite-frequency H_2 norm of the uncertain system. Imposing an initial guess for δ equal to 0, Table 1 reports the results yielded by the trust-region-reflective algorithm of *fmincon* and Algorithm 1. With equal accuracy, Algorithm 1 runs faster than *fmincon*.

Table 1. Results for the validation example.

	H_2 norm	δ	Computational Time	
			fmincon	Algorithm 1
Worst-case	0.944	0.25	$\approx 0.41\,\text{s}$	$\approx 0.07\,\text{s}$
Best-case	0.848	-1	$\approx 0.42\,\text{s}$	$\approx 0.06\,\text{s}$

The results of the table, furthermore, can be graphically visualized in Fig. 2, where the blue curves represent different realizations of the uncertain system and the worst (resp. best) finite-frequency H_2-norm condition identified by Algorithm 1 is depicted in red (resp. yellow). These results also confirm the accuracy of the guaranteed upper and lower bounds of Casati et al. (2024), equal to 0.950 and 0.844 respectively. The computational time for both bounds, however, is equal to 16.1 s in Casati et al. (2024), which is much larger than the time needed for the worst-case finite-frequency H_2-norm analysis. This is due to the fact that the guaranteed bounds are computed by solving time-consuming SDPs subject to LMIs.

Note eventually that similar results are obtained by choosing different initial equispaced frequency grids. Setting $N = 5, 50, 100$, in fact, Algorithm 1 yields the same finite-frequency H_2 norms and δ values of Table 1 with similar computational times. In this simple case, therefore, the algorithm is not particularly sensitive to the choice of the

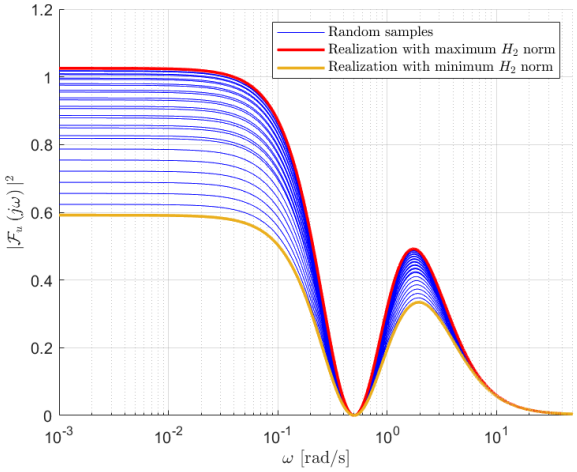

Fig. 2. Worst and best realizations: validation example.

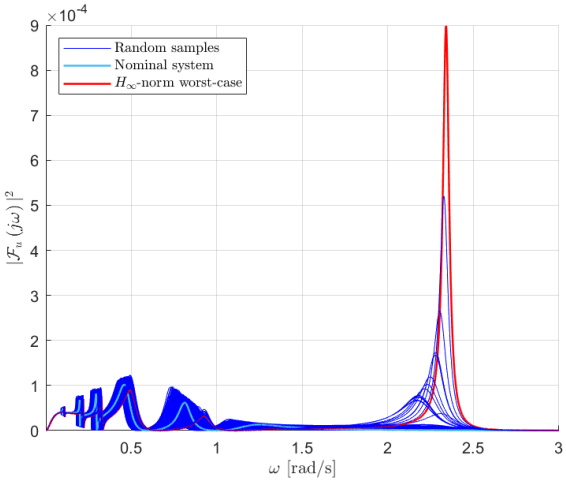

Fig. 3. Worst realization of the flexible satellite model with 17 uncertainties.

frequency grid. For more complex cases, however, it is reasonable to refine the frequency grid in the proximity of the transfer function's peaks.

5.2 Satellite Benchmark

The effectiveness of the proposed implementation is then tested on a more demanding single-axis satellite model taken from Roos et al. (2024). The transfer function between external disturbance and pointing angle is considered for H_2 performance. The benchmark is characterized by 17 uncertainties which can independently perturb the corresponding parameters up to $\pm 11\%$ their nominal values. The so-obtained LFT has 19 states and a $\mathbf{\Delta}$ matrix of size 22. The objective of the analysis is to determine a combination of uncertainties for which the finite-frequency H_2 norm of the LFT is maximum. A preliminary μ-based H_∞-norm analysis identifies a peak in $|\mathcal{F}_u(j\omega)|^2$ of about 9×10^4 at a frequency of 2.346 rad/s (see Roos et al. (2024)). Algorithm 1 is then run initializing $\mathbf{\Delta}_{wc}$ with the set of uncertainties corresponding to the realization yielding the worst H_∞ norm. $\overline{\omega}$ is set to 3 rad/s and $N = 10$ equispaced frequencies $\{\omega_k\}_{k=1,\dots,N}$ are selected between 0 rad/s and $\overline{\omega}$. An additional grid point, eventually, is added in correspondence of the worst H_∞ peak, namely at 2.346 rad/s. Algorithm 1 yields a worst-case finite-frequency H_2 norm of 5.4×10^{-3}, taking ≈ 0.07 s. The same result is provided by the trust-region-reflective algorithm of *fmincon* in ≈ 0.15 s. $\mathbf{\Delta}_{wc}$ is very similar to the set of uncertainties yielding the worst H_∞ norm, as the algorithms only provide a small step before stopping in a corner of the uncertainty domain. This result, however, is reasonable as the worst realization of the system in terms of finite-frequency H_2 norm coincides with the worst H_∞ case. This can be assessed in Fig. 3, which represents some samples of the uncertain system together with the realization yielding the worst H_∞ norm. This latter covers a larger area with respect to the blue curves and is therefore characterized by a higher finite-frequency H_2 norm.

5.3 MIMO H_2 Performance of a Spinning Satellite

Algorithm 1 is eventually tested on a MIMO continuous-time system with two inputs and two outputs. To do so, consider the model of a cylindrical satellite spinning around its axis of symmetry z with constant speed Ω taken from Somers et al. (2023). Torques T_x and T_y are used to control the angular rates ω_x and ω_y around the x and y axis respectively. Let also $I_x = I_y$ and I_z be the inertia of the satellite around its x, y and z axes. The rotational motion of the satellite is given by the following system of equations (Somers et al., 2023):

$$\begin{bmatrix} \dot{\omega}_x \\ \dot{\omega}_y \end{bmatrix} = \begin{bmatrix} 0 & a \\ -a & 0 \end{bmatrix} \begin{bmatrix} \omega_x \\ \omega_y \end{bmatrix} + \begin{bmatrix} \delta_1 & 0 \\ 0 & \delta_2 \end{bmatrix} \begin{bmatrix} u_x \\ u_y \end{bmatrix}$$

in feedback loop with the static control law:

$$\begin{bmatrix} u_x \\ u_y \end{bmatrix} = \begin{bmatrix} -1 - 0.5a & 0.5 - a \\ a & -1 \end{bmatrix} \begin{bmatrix} \omega_x \\ \omega_y \end{bmatrix} + \begin{bmatrix} r_x \\ r_y \end{bmatrix}$$

where $a = \Omega\left(1 - \dfrac{I_z}{I_x}\right)$, $u_x = \dfrac{T_x}{I_x}$, $u_y = \dfrac{T_y}{I_x}$, and δ_1, δ_2 are two uniformly distributed uncertain parameters representing possible variations of the control torques. The MIMO transfer function from the references r_x and r_y to the measurements $\begin{bmatrix} \nu_x \\ \nu_y \end{bmatrix} = \begin{bmatrix} 1 & a \\ -a & 1 \end{bmatrix} \begin{bmatrix} \omega_x \\ \omega_y \end{bmatrix}$ is considered for the analysis. Suppose that $a = 5$ and that both δ_1 and δ_2 can independently vary of 20% around their nominal values (equal to 1). The LFT is then normalized, $\overline{\omega}$ is set to 10 rad/s and $\{\omega_k\}_{k=1,\dots,N}$ are selected as the middle frequencies of $N = 10$ equispaced intervals $I(\omega_k)$ between 0 rad/s and $\overline{\omega}$. The trust-region-reflective algorithm of *fmincon* and Algorithm 1 are eventually run starting from nominal conditions (i.e. $\mathbf{\Delta} = \mathbf{0}$) and the obtained results are reported in Table 2. As in the previous examples, with the same accuracy Algorithm 1 runs faster than *fmincon*.

Table 2. Results for the spinning satellite.

	H_2 norm	J	τ	Computational Time	
				fmincon	Algorithm 1
Worst-case	5.57	-1	1	≈ 0.46 s	≈ 0.09 s
Best-case	3.29	-1	-1	≈ 0.46 s	≈ 0.10 s

The correctness of the identified worst and best-case conditions is proved by Fig. 4, which represents the surface plot of the finite-frequency H_2 norm with respect to the uncertainties in the system. This assesses the effectiveness

of the implemented algorithm also when applied to coupled MIMO systems. Note eventually that similar results are obtained with Algorithm 1 by setting $N = 5, 50, 100$. Not even in this case, therefore, is the algorithm sensitive to the initial choice of the frequency grid.

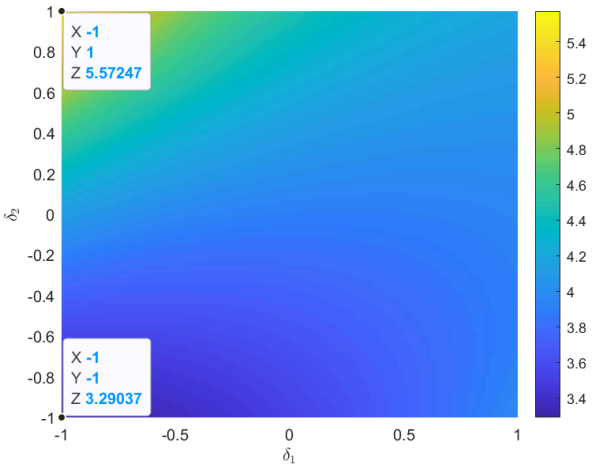

Fig. 4. Finite-frequency H_2 norm with respect to the uncertainties: spinning satellite.

6. CONCLUSIONS AND FUTURE WORK

The present paper proposes a new approach to identify worst-case (resp. best-case) finite-frequency H_2-norm conditions of linear systems in the presence of LTI real parametric uncertainties. The objective of the analysis is to determine a feasible combination of uncertainties which maximizes (resp. minimizes) the finite-frequency H_2 norm of the system. A major advantage of this approach is that it can equivalently be applied to SISO and MIMO models. Despite the fact that the algorithm may stop in a local optimum, it nonetheless yields a feasible combination of the uncertainties, which corresponds to an inner estimate of the worst (reps. best) finite-frequency H_2 norm. In order to increase the reliability of the results, it is also possible to run the algorithm starting from different initial conditions, including the realization yielding the worst-case H_∞ norm.

The results of this paper pave the way to many possible extensions and future work, specially when combined with the study of Casati et al. (2024). Worst-case finite-frequency H_2-norm conditions can indeed be computed much more rapidly than guaranteed bounds, which require solving multiple time-consuming SDPs subject to LMIs. The accuracy of the obtained upper (resp. lower) hard bounds can therefore be rapidly assessed by comparing them with the maximized (resp. minimized) finite-frequency H_2 norm. Furthermore, Algorithm 1 can be integrated into a Branch and Bound (B&B) scheme to accelerate the computation of hard bounds on the probability that the H_2 performance of an uncertain system either satisfies or violates a given requirement. The proposed worst-case finite-frequency H_2-norm analysis can also be extended to discrete-time systems, which is of particular interest in the context of hybrid multi-rate models (see Biannic et al. (2024)). Moreover, the knowledge of worst-case finite-frequency H_2-norm combinations of the uncertainties allows for a robust multimodel design of the AOCS yet in the early phases of the control synthesis. Eventually, further comparisons of Algorithm 1 with other optimization techniques should be carried out to confirm the effectiveness of the proposed approach.

REFERENCES

Biannic, J.M., Burlion, L., Demourant, F., Ferreres, G., Hardier, G., Loquen, T., and Roos, C. (2016). The SMAC Toolbox: a collection of libraries for Systems Modeling, Analysis and Control. URL `https://w3.onera.fr/smac/ssiqc`.

Biannic, J.M., Roos, C., and Cumer, C. (2024). LFT modelling and μ-based robust performance analysis of hybrid multi-rate control systems. In *Proceedings of the IEEE Conference on Decision and Control*. Milan, Italy.

Brito, A. and Kim, J. (2010). Application of a two-step calculation of the real structured singular value to the science mode of the LISA mission. In *Proceedings of the AIAA Guidance, Navigation, and Control Conference*. Toronto, Canada.

Casati, T., Roos, C., Biannic, J.M., and Evain, H. (2024). Guaranteed lower and upper bounds on the finite-frequency H_2 norm of uncertain linear systems. In *Proceedings of the IEEE Conference on Decision and Control*. Milan, Italy.

Ferreres, G. (1998). A μ analysis technique without frequency gridding. In *Proceedings of the American Control Conference*. Philadelphia, PA, USA.

Garulli, A., Hansson, A., Pakazad, S.K., Masi, A., and Wallin, R. (2013). Robust finite-frequency H_2 analysis of uncertain systems with application to flight comfort analysis. *Control Engineering Practice*, 21(5), 887–897.

Martin, M., Belien, F., Falke, A., and Förstner, R. (2021). Robust performance analysis using H_2-norm for quadcopter-based mobility on small bodies. In *Proceedings of the IEEE Aerospace Conference*. Big Sky, MT, USA.

Paganini, F. (1999). Convex methods for robust H_2 analysis of continuous-time systems. *IEEE Transactions on Automatic Control*, 44(2), 239–252.

Patartics, B., Seiler, P., Béla, T., and Vanek, B. (2023). Worst case uncertainty construction via multifrequency gain maximization with application to flutter control. *IEEE Transactions on Control Systems Technology*, 31(1), 155–165.

Roos, C. (2018). *Advanced control laws design and validation - A set of methods and tools to bridge the gap between theory and practice*. Habilitation à diriger des recherches, Université de Toulouse.

Roos, C., Biannic, J.M., and Evain, H. (2024). A new step towards the integration of probabilistic μ in the aerospace V&V process. *CEAS Space Journal*, 16, 59–71.

Somers, F., Roos, C., Sanfedino, F., Bennani, S., and Preda, V. (2023). Extension of probabilistic gain, phase, disk and delay margins for multi-input multi-output space control systems. In *Proceedings of the ESA GNC-ICATT*. Sopot, Poland.

Yazıcı, A., Karamancıoğlu, A., and Kasimbeyli, R. (2011). A nonlinear programming technique to compute a tight lower bound for the real structured singular value. *Optimization and Engineering*, 12(3), 445–458.